Study of the Time-Resolved Tryptophan Fluorescence of Crystalline α-Chymotrypsin†

Guido Desie, Noël Boens,* and Frans C. De Schryver
Department of Chemistry, Katholieke Universiteit Leuven, B-3030 Heverlee, Belgium
Received December 13, 1985; Revised Manuscript Received August 14, 1986

ABSTRACT: The tryptophan environments in crystalline α-chymotrypsin were investigated by fluorescence. The heterogeneous emission from this multitryptophan enzyme was resolved by time-correlated fluorescence spectroscopy. The fluorescence decays at 296-nm laser excitation and various emission wavelengths could be characterized by a triple-exponential function with decay times $\tau_1 = 150 \pm 50$ ps, $\tau_2 = 1.45 \pm 0.25$ ns, and $\tau_3 = 4.2 \pm 0.4$ ns. The corresponding decay-associated emission spectra of the three components had maxima at about 325, 332, and 343 nm. The three decay components in this enzyme can be correlated with X-ray crystallographic data [Birktoft, J. J., & Blow, D. M. (1972) *J. Mol. Biol. 68*, 187–240]. Inter- and intramolecular tryptophan–tryptophan energy-transfer efficiencies in crystalline α-chymotrypsin were computed from the accurately known positions and orientations of all tryptophan residues. These calculations indicate that the three fluorescence decay components in crystalline α-chymotrypsin can be assigned to three distinct classes of tryptophyl residues. Because of the different proximity of tryptophan residues to neighboring internal quenching groups, the decay times of the three classes are different. Decay time τ_1 can be assigned to Trp-172 and Trp-215 and τ_2 to Trp-51 and Trp-237, while the tryptophyl residues 27, 29, 141, and 207 all have decay time τ_3.

α-Chymotrypsin (α-CT),[1] a serine protease (Stroud, 1974; Blow, 1976; Kraut, 1977) containing eight tryptophan (Trp) residues, is one of the most thoroughly studied of all enzymes. A wide range of chemical, spectroscopic, and X-ray crystallographic studies has provided a detailed knowledge of the structure and catalytic mechanism of this important enzyme.

Fluorescence offers a very attractive method for investigating proteins (Beechem & Brand, 1985). The fluorescence characteristics of extrinsic probes have been used frequently to study the dynamics of α-CT in aqueous solution (Haugland & Stryer, 1967; Edelman & McClure, 1968; Schoellmann, 1972; Desie et al., 1986). The study of the intrinsic fluorescence of proteins has the advantage of measuring unperturbed biological systems. Of the 241 amino acid residues in α-CT, 6 are phenylalanyl (Phe) residues and 4 are tyrosinyl (Tyr) residues (Birktoft & Blow, 1972). Although both Phe and Tyr absorb at excitation wavelengths below ca. 290 nm, very little fluorescence is expected to originate from these residues because of their very low fluorescence quantum yields and the efficient long-range energy transfer to tryptophan (Teale, 1960; Longworth, 1968). Upon excitation above 295 nm, the observed fluorescence is expected to arise only from the tryptophyl residues. Thus, intrinsic time-resolved fluorescence is a very powerful tool for obtaining information about the tryptophan environments in this enzyme.

Several workers (Teale, 1960; Konev, 1967; Ivkova et al., 1968; Galley & Stryer, 1969) have reported the steady-state fluorescence properties (spectrum, bandwidth, quantum yield, maximum) of α-CT in aqueous solution. Recently, the intrinsic time-resolved fluorescence of this enzyme in aqueous solution has been reported (Maliwal & Lakowicz, 1984; Desie et al., 1985). Fucaloro and Forster (1985) have investigated the conformational fluctuations in α-chymotrypsinogen A powders. The fluorescence decays were analyzed as biexponential decay functions, and the mean decay time was determined as a function of hydration level.

In this paper, we present the results of a time-resolved study of the intrinsic fluorescence of crystalline α-CT. The heterogeneous steady-state fluorescence spectrum of this enzyme is separated by time-resolved emission spectroscopy into emission spectra from three temporally distinct components. The results are interpreted in terms of three distinct classes of tryptophyl residues, which are determined by proximity to neighboring internal quenching groups and energy transfer to other tryptophans.

Experimental Procedures

Materials. α-Chymotrypsin (EC 3.4.21.1) type I-S (from bovine pancreas, 3× crystallized, lyophilized, essentially salt free, Sigma C7762), *N*-acetyl-L-tryptophanamide (NATA, Sigma), and *p*-terphenyl (Merck, scintillator grade) were used as received. Xanthione, benzo[*b*]indeno[1,2-*e*]pyran (BIP), and stiff stilbene were synthesized and purified as described previously (Van den Zegel et al., 1986).

Instrumentation. Corrected excitation and fluorescence spectra of crystalline α-CT were obtained with a Spex Fluorolog 212/Datamate interfaced to a Digital Equipment Corp. PDP-11/23 computer (Desie & De Schryver, 1985). The samples were contained between two parallel quartz plates and measured in a temperature-controlled (22 ± 0.2 °C) cell holder in the front-phase configuration. Fluorescence decay curves were obtained by using the 296-nm excitation of a Spectra-Physics frequency-doubled, mode-locked, cavity-dumped, synchronously pumped R6G dye laser with time-correlated single photon counting detection (O'Connor & Phillips, 1984).

† G.D. was supported by the "Instituut ter bevordering van het Wetenschappelijk Onderzoek in de Nijverheid en de Landbouw" and the University of Leuven. N.B. is a Research Associate of the Fund for Medical Scientific Research (FGWO, Belgium). This work was supported by FGWO Grant 3.0099.86.

[1] Abbreviations: α-CT, α-chymotrypsin; BIP, benzo[*b*]indeno[1,2-*e*]pyran; DAS, decay-associated emission spectrum; NATA, *N*-acetyl-L-tryptophanamide.

0006-2960/86/0425-8301$01.50/0

The details of the fluorescence lifetime apparatus and the associated optical and electronic components are described elsewhere (Van den Zegel et al., 1986).

Fluorescence Decay Measurements: Data and Residual Analysis. The fluorescence decay measurements were performed by using the δ function convolution method (Zuker et al., 1985; Van den Zegel et al., 1986) to correct for the wavelength dependence of the shape of the instrument response function. This method requires the following: (1) a reference compound absorbs light at the same wavelength (λ_{ex}) and fluoresces at the same wavelength (λ_{em}) as that used for the sample; (2) the fluorescence δ response function of the reference compound is single exponential, i.e.

$$f_r(t) = \alpha_r \exp(-t/\tau_r) \quad (1)$$

where α_r is a preexponential factor and τ_r is the reference lifetime. The decay parameters of a modified decay function $\tilde{f}_s$ are obtained from the measured fluorescence decays of sample, D_s, and reference compound, D_r, observed at λ_{em}:

$$D_s = D_r \otimes \tilde{f}_s \quad (2)$$

where $\otimes$ denotes convolution. If the sample fluorescence δ response function can be written as a sum of exponentials, then $\tilde{f}_s$ becomes

$$\tilde{f}_s(t) = \sum_{j=1}^{k} \alpha_j/\alpha_r[\delta(0) + (1/\tau_r - 1/\tau_j) \exp(-t/\tau_j)] \quad (3)$$

where $\delta(0)$ is the Dirac δ function at zero, τ_j represents the sample decay times, and α_j/α_r is the preexponential. BIP in isooctane (λ_{em} = 350–400 nm, τ_r = 4 ps), stiff stilbene in dodecane (λ_{em} = 340–420 nm, τ_r = 12 ps), xanthione in isooctane (λ_{em} = 410–550 nm, τ_r = 43 ps), *p*-terphenyl in isooctane (λ_{em} = 320–400 nm, τ_r = 1.04 ns), and NATA in water (λ_{em} = 310–430 nm, τ_r = 2.98 ns) were used as reference compounds. Decays were collected in 256 or 512 channels of the multichannel analyzer. A reweighted iterative reconvolution method based on the algorithm of Marquardt (1963) was used to estimate the unknown parameters.

After a model function was fitted to the experimental fluorescence decay data, a careful inspection of the differences between observed and fitted decay data was made. The details of this residual analysis are given elsewhere (Boens et al., 1984; Desie et al., 1985; Van den Zegel et al., 1986). The graphical methods included residual plots, the autocorrelation function (Grinvald & Steinberg, 1974), and the normal probability plot. The numerical methods used to judge the goodness of fit were the calculation of the weighted sum of squared residuals and the reduced χ^2 and its standard normal deviate Zx^2. Fits with $|Zx^2| > 3$ were rejected. To examine the randomness of the time sequence of the residuals, the ordinary runs statistic Z was calculated. Fits with $|Z| > 3$ were considered unacceptable. The Durbin–Watson test statistic d was calculated to test for serial correlation between residuals. The tests for assessing the normality of the distribution of the error terms included the determination of the percentage of the residuals within the [−2,2] interval and the calculation of the mean (μ) and standard deviation (σ) of the residuals.

Decay-Associated Emission Spectra (DAS). The analysis of fluorescence decay curves as a function of emission wavelength allows the resolution of the steady-state emission spectrum into components associated with each decay time (Wahl & Auchet, 1972). The fluorescence spectra associated with the decay components (DAS) were obtained by scaling the $\alpha_j(\lambda)$ to the steady-state spectrum. For each emission wavelength, the steady-state intensity $I_{ss}(\lambda)$ must be the sum

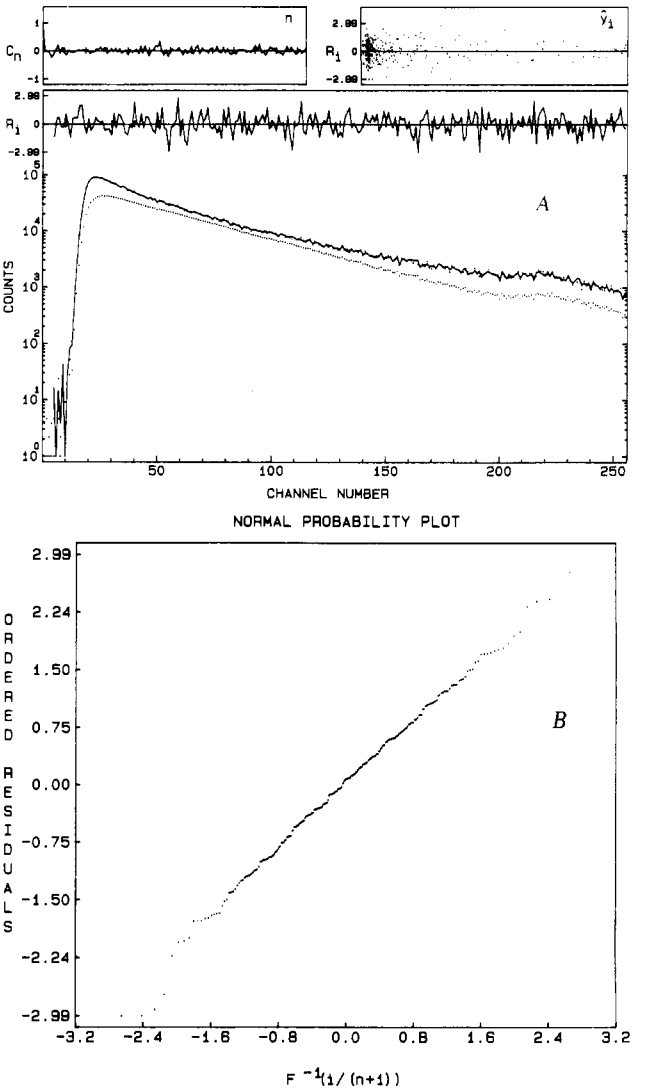

FIGURE 1: (A) Experimental fluorescence decay curve (point plot) of crystalline α-CT at 22 °C. The decay function calculated between channels 5 and 255 is shown as a solid line. The instrument response function (point plot) is the measured decay of NATA in water, pH 7. Also plotted are the autocorrelation function, C_n, and the weighted residuals R_i, vs. channel number, i, and vs. the calculated values $\hat{y}_i$. λ_{ex} = 296 nm; λ_{em} = 370 nm; channel width = 74 ps, peak channel counts = 91 965, total number of counts = 3 425 237. Estimated decay parameters: α_1 = 0.509, τ_1 = 153 ps, α_2 = 0.346, τ_2 = 1.563 ns, α_3 = 0.144, τ_3 = 4.381 ns, τ_r = 2.98 ns (constant). Test statistics: χ^2 = 1.08, Zx^2 = 0.90, Z = 0.02, d = 2.07, % = 95.51, μ = 0.00, σ = 1.04. (B) Normal probability plot corresponding to the analysis of Figure 1A.

of the intensities $I_j(\lambda)$ associated with each decay component. The intensity $I_j(\lambda)$ due to component j is given by

$$I_j(\lambda) = I_{ss}(\lambda)[\alpha_j\tau_j/\sum_j \alpha_j\tau_j] \quad (4)$$

RESULTS

Fluorescence Decay Analysis. The fluorescence decays (λ_{ex} = 296 nm) of crystalline α-CT at 22 °C could be analyzed adequately as a sum of three exponential terms with decay times of 150 ± 50 ps, 1.45 ± 0.25 ns, and 4.2 ± 0.4 ns. The same three decay times were found for analysis wavelengths ranging from 310 to 450 nm. An example of a three-component analysis and the corresponding normal probability plot are shown in Figure 1.

A satisfactory analysis in terms of three exponential components, however, does not necessarily imply that this model is the correct description of the data. Therefore, results of

Table I

(A) Results of Triple-Exponential Analysis of Fluorescence Decays of Crystalline α-CT at 22 °C as a Function of Number of Counts in Peak Channel[a]

peak channel counts	10000	30318	45767	84243	165946
total counts in decay	271319	1150317	1696690	3136577	6257222
α_1	0.705	0.495	0.587	0.564	0.550
τ_1 (ns)	0.132	0.152	0.114	0.121	0.118
α_2	0.242	0.356	0.289	0.300	0.312
τ_2 (ns)	1.375	1.568	1.560	1.525	1.518
α_3	0.053	0.149	0.124	0.136	0.138
τ_3 (ns)	4.206	4.404	4.324	4.263	4.292
χ^2	1.03	1.00	1.02	1.23	1.05
Zx^2	0.36	−0.02	0.23	2.59	0.51
Z	1.26	0.00	0.31	0.01	0.50
d	1.75	1.77	1.70	1.98	1.84
%	96.10	95.18	95.20	92.79	94.42
μ	0.06	0.07	0.07	0.00	0.00
σ	0.95	0.99	1.00	1.09	1.01
(B) Test Statistics of Double-Exponential Analysis of Fluorescence Decays of (A)					
χ^2	2.75	4.99	9.58	14.31	24.90
Zx^2	19.36	44.25	95.20	148.81	267.21
Z	−5.01	−9.28	−10.79	−9.94	−12.08
d	0.82	0.38	0.31	0.34	0.18
%	82.91	71.68	47.01	45.37	31.11
μ	0.41	0.37	0.51	0.52	0.66
σ	1.59	2.19	3.03	3.72	4.91

[a] NATA in water (pH 7) was used as reference compound. The reference lifetime was kept fixed at 2.98 ns in the curve-fitting calculation. λ_{ex} = 296 nm; λ_{em} = 370 nm; number of channels = 255; channel width = 74 ps.

triple-exponential fits should be carefully scrutinized and checked. Indeed, noise of the data can severely limit the ability of the various statistical tests to decide if a model is an accurate description of the experimental data (Van den Zegel et al., 1986). Increasing the number of counts makes the distinction (based on graphical and numerical statistical tests) between competing models clearer and diminishes the errors on the recovered parameters. Collecting data to a large number of counts with equipment free of common distortions and faults can therefore be helpful in choosing the correct functional form of the decay law and determining the need for additional terms in the decay function.

To examine the effect of increasing the signal to noise ratio, fluorescence decay curves were collected with the number of counts in the peak channel varying from 10 000 to 166 000. NATA in water, pH 7 (τ_r = 2.98 ns), was used as the reference compound. To account for instabilites in the equipment, sample and reference were measured alternately (Hazan et al., 1974). The results of the fluorescence decay data analyses as a double- and triple-exponential model are compiled in Table I as a function of the peak channel count. For the three-component analysis (Table IA), increasing the number of peak channel counts from 10 000 to 166 000 does not result in any improvement of the statistical parameters used to assess the quality of the fit, while the two-component analysis (Table IB) becomes progressively unacceptable with higher accumulated counts. The results show that at the 10 000 peak channel count level, the three decay components are easily resolvable. From the results presented in Table I, it is apparent that a double-exponential model is inadequate to describe the fluorescence decay of crystalline α-CT and that only a fit to three exponentials is satisfactory. Including an extra (fourth) exponential term in the decay law is not necessary since the F test (extra sum of squares principle; Draper & Smith, 1981; Ameloot & Hendrickx, 1982) is insignificant and the other statistical tests indicate no further improvement of the fit. Identical results were obtained for the double- and triple-exponential analyses of crystalline α-CT decay curves with between 5000 and 134 000 counts in the peak channel, and with p-terphenyl in isooctane (τ_r = 1.04 ns) as the reference emitter. The use of various reference emitters (stiff stilbene, BIP, xanthione, p-terphenyl, and NATA) in the δ function convolution technique gives the same values for the decay times τ_j and the fluorescence contributions $\alpha_j\tau_j/\sum\alpha_j\tau_j$. Further experimental evidence supporting a three-component fit includes the emission wavelength independence of the decay times and the temperature dependence (unpublished experiments) of the decay components. Analyses of decay curves obtained with vertically plane-polarized excitation light (Spectra-Physics Model 310A broadband polarization rotator inserted in the excitation beam) and detection through a polarizer set at 0° (vertical), 54°44′ (magic angle), or 90° (horizontal) with respect to the vertical laboratory axis all gave identical results. The same decays were obtained with horizontally plane-polarized light and with fluorescence detected with or without the polarizer. The angle of rotation of the polarizer did not have any influence on the recovered decay parameters. Varying the channel time increment and/or the number of data channels did not influence the recovered decay parameters.

The steady-state fluorescence spectrum of crystalline α-CT and the decay parameters α_j and τ_j determined from triple-exponential decay analyses at emission wavelengths from 310 to 450 nm were used to calculate the emission spectra associated with the three decay components (DAS, eq 4). The DAS of crystalline α-CT are shown in Figure 2.

Tryptophan–Tryptophan Energy-Transfer Efficiencies. Because the absorption and emission envelopes of the individual Trp residues in crystalline α-CT cannot be determined separately, calculations of Trp–Trp energy-transfer efficiencies will be subject to some uncertainty.

However, realistic upper and lower values for the overlap integral J_{AD} (eq 5) can be obtained by combining the most

$$J_{AD} = \int F_D(\lambda)\epsilon_A(\lambda)\lambda^4\, d\lambda / \int F_D(\lambda)\, d\lambda \qquad (5)$$

hypsochromic fluorescence spectra of Trp-containing proteins with the most hyperchromic absorption spectra, and the most bathochromic fluorescence spectra with the most hypochromic absorption spectra, respectively (Teale, 1960). Using these

Table II: Intramolecular Trp–Trp Energy-Transfer Efficiencies in Crystalline Monomeric α-CT[a]

$^1L_a/^1L_a$	27	29	51	141	172	207	215	237
27	1.00	0.71	0.00	0.44	0.00	0.02	0.02	0.02
29	0.71	1.00	0.15	0.53	0.02	0.96	0.01	0.07
51	0.00	0.15	1.00	0.05	0.00	0.03	0.02	0.06
141	0.44	0.53	0.05	1.00	0.00	0.08	0.02	0.03
172	0.00	0.02	0.00	0.00	1.00	0.05	0.97	0.02
207	0.02	0.96	0.03	0.08	0.05	1.00	0.01	0.04
215	0.02	0.01	0.02	0.02	0.97	0.01	1.00	0.12
237	0.02	0.07	0.06	0.03	0.02	0.04	0.12	1.00
$^1L_a/^1L_b$	27	29	51	141	172	207	215	237
27	1.00	0.99	0.03	0.29	0.01	0.04	0.01	0.00
29	0.85	1.00	0.00	0.02	0.01	0.91	0.04	0.02
51	0.00	0.01	1.00	0.01	0.00	0.00	0.01	0.79
141	0.41	0.34	0.06	1.00	0.00	0.09	0.05	0.03
172	0.01	0.02	0.00	0.00	1.00	0.00	0.82	0.00
207	0.56	0.83	0.00	0.07	0.00	1.00	0.00	0.00
215	0.01	0.00	0.00	0.01	0.98	0.02	1.00	0.01
237	0.01	0.01	0.75	0.00	0.00	0.03	0.01	1.00
$^1L_b/^1L_b$	27	29	51	141	172	207	215	237
27	1.00	0.90	0.08	0.72	0.00	0.97	0.00	0.01
29	0.90	1.00	0.36	0.28	0.00	0.98	0.00	0.03
51	0.08	0.36	1.00	0.03	0.00	0.07	0.01	0.04
141	0.72	0.28	0.03	1.00	0.04	0.02	0.07	0.00
172	0.00	0.00	0.00	0.04	1.00	0.00	0.99	0.01
207	0.97	0.98	0.07	0.02	0.00	1.00	0.00	0.00
215	0.00	0.00	0.01	0.07	0.99	0.00	1.00	0.06
237	0.01	0.03	0.04	0.00	0.01	0.00	0.06	1.00

[a] Values are listed for the $^1L_a \leftarrow {}^1L_a$, $^1L_a \leftarrow {}^1L_b$, $^1L_b \leftarrow {}^1L_a$, and $^1L_b \leftarrow {}^1L_b$ transitions.

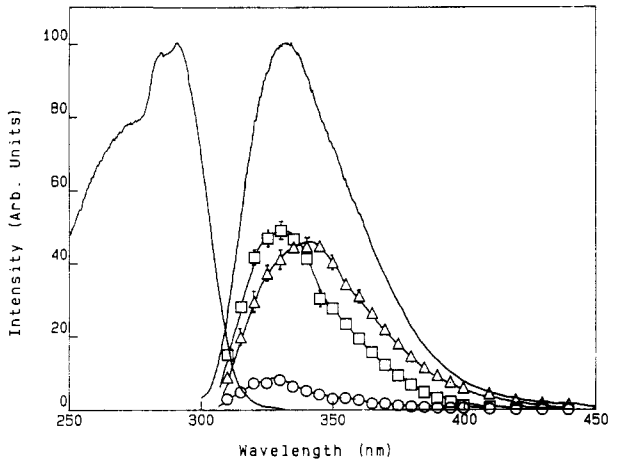

FIGURE 2: Decay-associated emission spectra of crystalline α-CT. (Upper curve) Steady-state spectrum, excitation at 296 nm (0.9-nm band-pass). DAS of component 1, τ_1 = 150 ps (○); component 2, τ_2 = 1.45 ns (□); component 3, τ_3 = 4.2 ns (△). Spectra were constructed according to eq 4. Error bars are propagated errors computed from the standard errors of α_j/α_r and τ_j. When no error bars are given, errors are within the contours of the plotted symbols. The excitation spectrum of crystalline α-CT (emission at 350 nm) is also shown.

extreme data, we calculated respective minimum and maximum values of 7.3×10^{-17} cm^6 mmol^{-1} and 4.3×10^{-16} cm^6 mmol^{-1} for the Trp–Trp spectral overlap integral J_{AD}. Assuming that the oscillator strengths in solution and crystalline α-CT are the same, a value of 2.4×10^{-16} cm^6 mmol^{-1} was found for the spectral overlap integral J_{AD} of a single tryptophyl residue in crystalline α-CT. This value is in excellent agreement with the J_{AD} value (2.1×10^{-16} cm^6 mmol^{-1}) calculated for NATA in tris(hydroxymethyl)aminomethane buffer, pH 7.8. In eq 5, $F_D(\lambda)$ denotes the fluorescence intensity of the donor at wavelength λ and $\epsilon_A(\lambda)$ the molar extinction coefficient of the acceptor at the same wavelength.

The Förster critical distance, R_0 (eq 6), the distance at which the rate of energy transfer between donor and accepter is equal to the sum of all other modes of deactivation of the donor, is given by (Förster, 1948, 1965)

$$R_0 = 9.79 \times 10^3 (J_{AD} n^{-4} \kappa^2 \Phi_D)^{1/6} \text{ Å} \quad (6)$$

In eq 6, J_{AD} denotes the spectral overlap integral (eq 5), n the refractive index of the medium, κ^2 the dipole–dipole orientation factor, and Φ_D the donor fluorescence quantum yield in the absence of accepter.

Values of the orientation factor κ^2 were calculated explicitly for each Trp–Trp pair according to eq 7:

$$\kappa^2 = [\cos \theta_t - 3 \cos \theta_D \cos \theta_A]^2 \quad (7)$$

In eq 7, θ_t is the angle between the donor and acceptor dipole vectors; θ_D and θ_A are the angles between the direction vector and the donor and accepter transition dipole vectors, respectively. The near-ultraviolet absorption band of indole and related compounds involves the overlapping ^1L_a and ^1L_b transitions (Valeur & Weber, 1977). Fluorescence also was attributed to these two different emitting states (Schütt & Zimmermann, 1963). Obtaining a single value for κ^2 is thus impossible since four combinations of transitions ($^1L_a \leftarrow {}^1L_a$, $^1L_a \leftarrow {}^1L_b$, $^1L_b \leftarrow {}^1L_a$, and $^1L_b \leftarrow {}^1L_b$) are possible. We computed κ^2 values for these transitions between all Trp–Trp pairs. It was assumed that the transition moment direction of ^1L_b makes an angle of 54° to the long axis of the indole molecule, while that of ^1L_a lies at an angle of −38° to the same axis (Yamamoto & Tanaka, 1972). After substitution in eq 6 of the κ^2 values (eq 7), 0.14 for the fluorescence quantum yield (Φ_D) of crystalline α-CT, 1.5 for the refractive index (n), and 2.4×10^{-16} cm^6 mmol^{-1} for J_{AD}, R_0 values were calculated for the transitions between any Trp–Trp pair. The efficiencies (E) (eq 8) for dipole–dipole energy transfer between tryptophyl

$$E = R_0^6/(R_0^6 + R^6) \quad (8)$$

residues in crystalline monomeric α-CT were calculated from the Trp–Trp distances R and the R_0 values obtained as described above. These efficiencies are compiled in Table II.

From the calculations for the $^1L_a \leftarrow {}^1L_b$ and $^1L_b \leftarrow {}^1L_a$ transitions (Table II), it is evident that the efficiency of energy

migration among the tryptophyl residues 27, 29, 141, and 207 is very high. The same is true for residues 51 and 237 and for residues 172 and 215. Upon excitation of the Trp residues in crystalline α-CT, the excitation energy is thus transferred very effectively among different Trp residues within one class, while transfer from one class to another is negligibly small. The calculations of energy-transfer efficiencies between ^1L_a and ^1L_b transitions indicate that the intrinsic fluorescence of the enzyme can be attributed to emission from three different independent classes.

The calculations for the $^1L_a \leftarrow {}^1L_a$ and $^1L_b \leftarrow {}^1L_b$ transitions show that Trp-172 and Trp-215 form a single class. Residues 27, 29, 141, and 207 transfer the excitation energy very effectively among them, while there is some energy transfer to Trp-51. Trp-237 is an individual residue which does not interact with any other Trp. These data are also compatible with the existence of three classes: Trp residues 27, 29, 141, and 207 form one class which is coupled weakly to residue 51; Trp-172 and Trp-215 comprise a second class; the individual Trp-237 forms the third class.

Since the absorption and emission of tryptophyl compounds involve the overlapping ^1L_a and ^1L_b bands (Valeur & Weber, 1977; Schütt & Zimmermann, 1963), the actual Trp–Trp interaction will be a combination of the energy-transfer efficiencies listed in Table II. These results support the classification of the Trp residues in crystalline α-CT into three classes: one class consists of Trp residues 27, 29, 141, and 207, the second class comprises Trp-51 and Trp-237, and the third class is formed by the Trp pair 172 and 215.

Since the Trp–Trp distances between neighboring α-CT molecules in the crystal lattice can be small enough for efficient *inter*molecular energy transfer, this effect has to be included in the calculations of the energy-transfer efficiencies. Crystalline α-CT contains two molecules in the crystallographic asymmetric unit, giving rise to a system of local (or noncrystallographic) 2-fold axes within the crystal structure. These local 2-fold axes are exactly perpendicular to the crystallographic *b* and *c* axes (Briktoft & Blow, 1972). The existence of local dyed axes (related by crystallographic symmetry) requires that the *inter*molecular interactions of the Trp residues have to be checked for two crystallographically distinct α-CT molecules of the four present in the $P2_1$ unit cell. For each of these 2 different α-CT molecules, the effect of its 26 neighbors was investigated (8 in the same crystal plane, 9 above and 9 under that plane). Molecule 1 [classification of Birktoft & Blow (1972)] can interact with molecules 2 and 4. All possible interactions between the ^1L_a and ^1L_b transitions were investigated. The *inter*molecular energy-transfer efficiency is high between the tryptophyl residues 172 and 215 of molecules 1 and 2, which supports the classification of these residues as one class in crystalline α-CT. There is also a small *inter*molecular energy transfer between the Trp residues 237 in molecules 1 and 4. It should be noted that the remaining Trp residues of molecule 1 do not show any *inter*molecular energy transfer. Low energy-transfer efficiencies are observed for the tryptophyl residues 29, 51, 207, and 237 in molecules 3 and 6. Molecule 6 is the upper neighbor of molecule 3 of Birktoft and Blow (1972). Because of symmetry, energy-transfer efficiencies for Trp residues in molecules 2 and 4 of the unit cell can be obtained from those of molecules 1 and 3.

Discussion

The ability of accurately resolving complex fluorescence decays depends critically upon various factors. The essential condition for obtaining reliable decay parameter estimates is the measurement of good quality data. Thus, the time-correlated single photon counting fluorescence decays should be recorded in such a manner that all commonly found distortions and errors are avoided or can be corrected for (Boens et al., 1986). As much as possible, it is preferable to eliminate experimental distortions by instrumental techniques rather than to correct for them in data analysis (O'Connor & Phillips, 1984). Since the convolution model has been found to have a low intrinsic nonlinearity (Ameloot & Hendrickx, 1982), model evaluation can be done, relying on the methods of linear regression. Consequently, the χ^2 (Zx^2) test (lack of fit) and the *F* test (extra sum of squares; Draper & Smith, 1981) can be used to decide if extra exponential terms have to be included in the model. Because the error distribution of the experimental time-correlated single photon counting fluorescence decay data is well-known, a proper statistical assessment of the quality of fit can be made. The use of the δ function convolution technique (Zuker et al., 1985; Van den Zegel et al., 1986) to correct effectively for the wavelength variation of the instrument response function eliminates the main cause for poor fits in time-correlated single photon fluorescence decay measurement. A low signal to noise ratio, i.e., low counts per channel, and/or insufficient dynamic range of the decay data can mask a more complex underlying model. Collecting good quality data to a large number of counts can eventually reveal the presence of a more complicated decay law. A final factor determining the accuracy of estimated fluorescence decay parameters is the statistical methodology employed in the data analysis. Critical comparisons (McKinnon et al., 1977; O'Connor et al., 1979) of the analysis methods of fluorescence decay data indicate that the nonlinear least-squares iterative reconvolution (Marquardt, 1963; Bard, 1974) is the most suitable.

Measuring fluorescence decays on a time-correlated single photon counting apparatus free of all commonly found distortions (Boens et al., 1986) ensured that good quality data were obtained. This is substantiated by the adequate fits obtained with the nonlinear least-squares reweighted (Zuker et al., 1985; Van den Zegel et al., 1986) iterative reconvolution based on the Marquardt (1963) algorithm. The rigorous analysis of the residuals clearly indicates that a three-component fit with decay times of 150 ± 50 ps, 1.45 ± 0.25 ns, and 4.2 ± 0.4 ns is the best description of the time-resolved fluorescence of crystalline α-CT at 22 °C. A triple-exponential model fit is the best at all precision levels. Indeed, increasing the number of counts in the peak channel from 10000 to 166000 (Table I and Figure 1) shows that no hidden decay components go undetected at the low count levels. The increasingly unsatisfactory double-exponential fits and the constantly acceptable triple-exponential fits (Table I and the results with *p*-terphenyl as reference) as a function of the number of accumulated counts are a reliable indication (Van den Zegel et al., 1986) that a three-component model is the adequate description of the decay data.

The DAS given in Figure 2 exhibit a bathochromic shift with increasing decay time. The corresponding maxima are at about 325, 332, and 343 nm. That the emission spectra associated with the longer decay times are more red-shifted has been reported [see Beechem & Brand (1985) and references cited therein] for tryptophan, *lac* repressor, horse liver alcohol dehydrogenase, yeast 3-phosphoglycerate kinase, myosin subfragment 1, terminal deoxynucleotidyl transferase (Robbins et al., 1985), and α-chymotrypsin in aqueous buffer (Desie et al., 1985).

It is popular in the literature [see Beechem & Brand (1985) and references cited therein] to resolve the complex fluorescence decays of multitryptophan proteins in terms of individual tryptophan or classes of Trp residues. Each class would then have a distinct decay time and spectral distribution. The correct calculation of energy-transfer efficiencies between pairs of tryptophans clearly supports the existence of three classes of Trp residues in crystalline α-CT. Since the near-ultraviolet excitation and the corresponding emission of tryptophyl compounds involve the overlapping ^1L_a and ^1L_b transitions (Valeur & Weber, 1977; Schütt & Zimmermann, 1963), the most plausible classification of the Trp residues of crystalline α-CT is as follows: Trp-27, -29, -141, and -207 form one class, Trp-51 and -237 are the members of the second class, and the Trp pair 172 and 215 comprise the third class. Can these groups of Trp residues be associated with the decay times? On the basis of the X-ray crystal structure analysis of α-CT and the results presented here, we believe that an assignment of the three classes of Trp residues to the decay times is feasible. This assignment is in agreement with studies of the pH dependence and the solute and thermal quenching of the different components of the time-resolved fluorescence of α-CT in aqueous buffer solution. The fluorescence properties of α-CT under denaturing conditions also support this assignment. The results of these experiments will be published separately.

The crystal structure analysis of α-CT shows that the indole nitrogens of Trp-172 and -215 are inaccessible to both externally and internally bound water molecules. Only the six-membered ring of the side group of Trp-172 is exposed to external water on one side.

The indole N of Trp-51 forms hydrogen bonds with two (external) water molecules (W-27 and W-42; Birktoft & Blow, 1972). Only the indole N and the adjacent C-2 of the side chains of Trp-51 and -237 are accessible to external water.

The side groups of Trp-27 and -29 and the indole N of Trp-141 are inaccessible to external water. The indole N of Trp-29 and the Trp-141 NH form hydrogen bonds with internal water molecules (W-8 and W-6, respectively). C-7 of the side group of Trp-141 is in contact with water molecules W-16 (surface) and W-17 (internal). The indole N of Trp-207 is accessible to external water.

Because the tryptophan emission is sensitive to solvent accessibility and polarity, information about the local environments of Trp residues in proteins may be revealed. The data given in the previous sections indicate clearly that the local environment of the Trp residues 172 and 215 is the most hydrophobic of all. We can thus safely attribute the most hypsochromic emission spectrum associated with $\tau_1 = 150$ ps to Trp-172 and -215. Since the Trp residues of the other two classes are more accessible to water, their DAS will be the more bathochromic ones. On the basis of accessibility of the tryptophans to water, it is impossible to predict to which class the decay-associated emission spectrum may be assigned to.

Since the two bathochromic decay-associated emission spectra could not be assigned unequivocally to the two remaining classes, we tried to link their decay times to the Trp residue classes. Therefore, we computed the shortest distances between the eight indole groups of crystalline α-CT and all possible internal quenching groups. There is overwhelming evidence that the emission of indole and related compounds is efficiently quenched by carbonyl compounds (Cowgill, 1963; Ricci & Nesta, 1976; Fleming et al., 1978; Werner & Forster, 1979; Bohorquez et al., 1984), arginine (Arg), cysteine (Cys), methionine (Met) (Bushueva et al., 1975), and ammonium groups (Ricci, 1970; Bushueva et al., 1975; Robbins et al., 1980; Szabo & Rayner, 1980; Chang et al., 1983). The close proximity of ammonium and carbonyl groups to the indole group has been invoked by many researchers (Werner & Forster, 1979; Szabo & Rayner, 1980; Chang et al., 1983; Petrich et al., 1983) to account for the different fluorescence lifetimes found for tryptophan and tryptophyl derivatives.

The indole N of Trp-172 forms a hydrogen bond with the carbonyl group of proline-225 (Pro-225) (at 3.1 Å). The quenching resulting from electron transfer to the Pro carbonyl accepter is enhanced by the close proximity of the ϵ-ammonium group of lysine-175 (Lys-175). This group is located at 5.5 Å from the indole ring of Trp-172. An analogous interaction exists for Trp-215: the shortest distances of the indole ring of Trp-215 to the ϵ-ammonium groups of Lys-175 and -177 are 6.1 and 8.3 Å, respectively. Furthermore, the Met-180 S forms a hydrogen bond (at 3.8 Å) with the indole N of Trp-215. Both Trp residues are thus quenched very effectively, resulting in a very short decay time for this class. These data support the assignment of the most hypsochromic class to the 150-ps component.

In the class consisting of Trp residues 51 and 237, the latter residue is not affected by intramolecular quenching groups. The indole group of Trp-51 is located at 4 Å from the ϵ-ammonium group of Lys-107 and the α-carboxyl group of Asn-245. Since only one Trp residue in this class is quenched efficiently, this class should be assigned to the 1.45-ns component.

In the class consisting of Trp-27, -29, -141, and -207, the distance between the indole ring of Trp-141 and the carbonyl group of Phe-71 is 2.9 Å. Since the carbonyl group of Phe-71 is not activated by a nearby ammonium group, only a moderate quenching is expected. The ϵ-ammonium group of Lys-202 and the indole group of Trp-207 are at 4.5 Å. There is no electron accepter at short distance from Trp-207. Its decay time will be reduced via a direct charge transfer mechanism (Chang et al., 1983). Since only one Trp residue in this class is quenched effectively, a large mean decay time is expected to be found for this class. The 4.2-ns component can thus be attributed to emission from the most bathochromic Trp residues 27, 29, 141, and 207.

α-CT is an example of a protein where the most hydrophobic tryptophans (172 and 215) are located near the surface of the enzyme, while the most hydrophilic tryptophan environment (Trp-27, -29, -141, and -207) is buried within the core of the protein. The 1.45-ns component (Trp-51 and -237, maximum 332 nm) is an exposed hydrophilic tryptophan environment. An analogous enzyme is terminal deoxynucleotidyl transferase (Robbins et al., 1985). The study of α-CT demonstrates that the environment of surface Trp residues is not necessarily the most polar. Indeed, if the buried Trp residues are more exposed to (internal) water molecules than the Trp residues near the surface of the enzyme, the buried Trp residues can exhibit a more bathochromic emission. A correlation between the polarity of the Trp environment and surface or buried Trp residues can only be made when additional information (e.g., from quenching experiments or structure analysis) is available.

The origin of single or multiexponential decay kinetics of the intrinsic tryptophyl fluorescence of polypeptides and proteins continues to be a topic of research and discussion. While indole and several indole derivatives such as 1-methylindole, 3-methylindole, 1,2-dimethylindole, and NATA exhibit single-exponential decay behavior in solution, a biexponential is necessary to describe the fluorescence decay of zwitterionic tryptophan. Since none of the eight Trp residues in α-CT is an end amino acid, the explanation for the biex-

ponential decay of zwitterionic tryptophan (Szabo & Rayner, 1980; Chang et al., 1983; Petrich et al., 1983) cannot be used to account for the triple-exponential fluorescence decay of α-CT. Many polypeptide hormones and proteins with a single tryptophan residue exhibit multiple fluorescence decay times [see Beechem & Brand (1985) and references cited therein]. The multiexponential fluorescence decays can be rationalized in terms of local microheterogeneity (conformers). Impurities can also be the cause for extra exponential terms: while Grinvald and Steinberg (1976) measured a double-exponential decay for RNase T1 (single Trp enzyme), an extensively purified sample exhibits single-exponential fluorescence decay (James et al., 1985). The emission of multitryptophan proteins is also complex [see Beechem & Brand (1985) and references cited therein]. However, the number of exponentials is usually equal to or smaller than the number of Trp residues. Trp residues at a short distance from each other and with the proper orientation transfer their excitation energy very efficiently, resulting in a single decay time (Formoso & Forster, 1975). When internal quenching side groups are present at a short distance from the fluorophore, the decay time of this fluorescent residue will be reduced considerably (Ross et al., 1986). When a protein exists in different conformations during the fluorescence time scale, the local Trp environments of all Trp residues in all conformations have to be taken into account.

This study shows that, if the Trp environments within a protein are accurately known (e.g, from X-ray crystallographic analysis, two-dimensional NMR studies, etc.), the emission characteristics of a protein can even be predicted. Time-resolved fluorescence studies of the Trp residues of proteins of known structure can therefore contribute significantly to our understanding of the usually complex fluorescence decay behavior. Once the relation between protein structure and emission is known for a number of well-characterized proteins, the intrinsic fluorescence will offer an attractive method for obtaining *precise* information about proteins of *unknown* structure.

Registry No. α-CT, 9004-07-3; L-Trp, 73-22-3.

REFERENCES

Ameloot, M., & Hendrickx, H. (1982) *J. Chem. Phys. 76*, 4419–4432.

Bard, Y. (1974) *Nonlinear Parameter Estimation*, Academic Press, New York.

Beechem, J. M., & Brand, L. (1985) *Annu. Rev. Biochem. 54*, 43–71.

Birktoft, J. J., & Blow, D. M. (1972) *J. Mol. Biol. 68*, 187–240.

Blow, D. M. (1976) *Acc. Chem. Res. 9*, 145–152.

Boens, N., Van den Zegel, M., & De Schryver, F. C. (1984) *Chem. Phys. Lett. 111*, 340–346.

Boens, N., Van den Zegel, M., De Schryver, F. C., & Desie, G. (1986) *Photobiochem. Photobiophys.* (in press).

Bohorquez, M. Del V., Cosa, J. J., Garcia, N. A., & Previtali, C. M. (1984) *Photochem. Photobiol. 40*, 201–205.

Bushueva, T. L., Busel, E. P., & Burstein, E. A. (1975) *Stud. Biophys. 52*, 41–52.

Chang, M. C., Petrich, J. W., McDonald, D. B., & Fleming, G. R. (1983) *J. Am. Chem. Soc. 105*, 3819–3824.

Cowgill, R. W. (1963) *Arch. Biochem. Biophys. 100*, 36–44.

Desie, G., & De Schryver, F. C. (1985) *Instrum. Comput. 3*, 44–52.

Desie, G., Boens, N., Van den Zegel, M., & De Schryver, F. C. (1985) *Anal. Chim. Acta 170*, 45–59.

Desie, G., Van Deynse, D., & De Schryver, F. C. (1986) *Photochem. Photobiol.* (in press).

Draper, N. R., & Smith, H. (1981) *Applied Regression Analysis*, 2nd ed., Wiley, New York.

Edelman, G. M., & McClure, W. O. (1968) *Acc. Chem. Res. 1*, 65–70.

Fleming, G. R., Morris, J. M., Robbins, R. J., Woolfe, G. J., Thistlethwaite, P. J., & Robinson, G. W. (1978) *Proc. Natl. Acad. Sci. U.S.A. 75*, 4642–4656.

Formoso, C., & Forster, L. S. (1975) *J. Biol. Chem. 250*, 3738–3745.

Förster, T. (1948) *Ann. Phys. (Leipzig) 2*, 55–75.

Förster, T. (1965) in *Modern Quantum Chemistry* (Sinanoglu, O., Ed.) pp 93–137, Academic Press, New York.

Fucaloro, A. F., & Forster, L. S. (1985) *Photochem. Photobiol. 41*, 91–93.

Galley, W. C., & Stryer, L. (1969) *Biochemistry 8*, 1831–1838.

Grinvald, A., & Steinberg, I. Z. (1974) *Anal. Biochem. 59*, 583–598.

Grinvald, A., & Steinberg, I. Z. (1976) *Biochim. Biophys. Acta 427*, 663–678.

Haugland, R. P., & Stryer, L. (1967) in *Conformation of Biopolymers* (Ramachandran, G. N., Ed.) Vol. 1, pp 321–335, Academic Press, New York.

Hazan, G., Grinvald, A., Maytal, M., & Steinberg, I. Z. (1974) *Rev. Sci. Instrum. 45*, 1602–1604.

Ivkova, M. N., Mosolov, V. V., & Burshtein, E. A. (1968) *Mol. Biol. 2*, 661–666.

James, D. R., Demmer, D. R., Steer, R. P., & Verrall, R. E. (1985) *Biochemistry 24*, 5517–5526.

Konev, S. V. (1967) *Fluorescence and Phosphorescence of Proteins and Nucleic Acids*, Plenum Press, New York.

Kraut, J. (1977) *Annu. Rev. Biochem. 46*, 331–358.

Longworth, J. W. (1968) *Photochem. Photobiol. 7*, 587–596.

Maliwal, B. P., & Lakowicz, J. R. (1984) *Biophys. Chem. 19*, 337–344.

Marquardt, D. W. (1963) *J. Soc. Ind. Appl. Math. 11*, 431–441.

McKinnon, A. E., Szabo, A. G., & Miller, D. R. (1977) *J. Phys. Chem. 81*, 1564–1570.

O'Connor, D. V., & Phillips, D. (1984) *Time-Correlated Single Photon Counting*, Academic Press, London.

O'Connor, D. V., Ware, W. R., & Andre, J. C. (1979) *J. Phys. Chem. 83*, 1333–1343.

Petrich, J. W., Chang, M. C., McDonald, D. B., & Fleming, G. R. (1983) *J. Am. Chem. Soc. 105*, 3824–3832.

Ricci, R. W. (1970) *Photochem. Photobiol. 12*, 67–75.

Ricci, R. W., & Nesta, J. M. (1976) *J. Phys. Chem. 80*, 974–980.

Robbins, D. J., Deibel, M. R., Jr., & Barkley, M. D. (1985) *Biochemistry 24*, 7250–7257.

Robbins, R. J., Fleming, G. R., Beddard, G. S., Robinson, G. W., Thistlethwaite, P. J., & Woolfe, G. J. (1980) *J. Am. Chem. Soc. 102*, 6271–6279.

Ross, J. B. A., Laws, W. R., Buku, A., Sutherland, J. C., & Wyssbrod, H. R. (1986) *Biochemistry 25*, 607–612.

Schoellmann, G. (1972) *Int. J. Pept. Protein Res. 4*, 221–227.

Schütt, H. U., & Zimmermann, H. (1963) *Z. Elektrochem. 67*, 54–62.

Stroud, R. M. (1974) *Sci. Am. 231*, 74–88.

Szabo, A. G., & Rayner, D. M. (1980) *J. Am. Chem. Soc. 102*, 554–563.

Teale, F. W. J. (1960) *Biochem. J. 76*, 381–388.

Valeur, B., & Weber, G. (1977) *Photochem. Photobiol. 25*, 441–444.

Van den Zegel, M., Boens, N., Daems, D., & De Schryver, F. C. (1986) *Chem. Phys. 101*, 311–335.
Wahl, P., & Auchet, J. C. (1972) *Biochim. Biophys. Acta 285*, 99–117.
Werner, T. C., & Forster, L. S. (1979) *Photochem. Photobiol. 29*, 905–914.
Yamamoto, Y., & Tanaka, J. (1972) *Bull. Chem. Soc. Jpn. 45*, 1362–1366.
Zimmermann, H., & Joop, N. (1961) *Z. Elektrochem. 65*, 61–65.
Zuker, M., Szabo, A. G., Bramall, L., Krajcarski, D. T., & Selinger, B. (1985) *Rev. Sci. Instrum. 56*, 14–22.

Dissociation of the Lactose Repressor Protein Tetramer Using High Hydrostatic Pressure†

Catherine A. Royer‡ and Gregorio Weber*
School of Chemical Sciences, Department of Chemistry, University of Illinois at Urbana-Champaign, Urbana, Illinois 61801
Thomas J. Daly and Kathleen Shive Matthews
Department of Biochemistry, Rice University, Houston, Texas 77251
Received April 4, 1986; Revised Manuscript Received July 14, 1986

ABSTRACT: Dissociation of *lac* repressor tetramer by high hydrostatic pressures was monitored with intrinsic tryptophan fluorescence. With the assumption of complete dissociation to monomer, tryptophan polarization data gave $\Delta V_a \sim 170$ mL/mol and the concentration for 50% tetramer dissociation, $C_{1/2}$, was 3.8×10^{-8} M. Upon addition of inducer, the calculated ΔV_a increased to ~220 mL/mol and the $C_{1/2}$ decreased to approximately 1×10^{-8} M, a free energy difference of ~0.7 kcal. These results indicate a modest stabilization of the tetramer by the presence of inducer. Monitoring the average energy of tryptophan emission demonstrated that (1) tetramer dissociation takes place over the same range of pressures as evidenced by the polarization data and (2) IPTG dissociation can be more or less superimposed upon tetramer dissociation depending upon the ligand concentration used. Although the two transitions cannot be separated entirely, the ΔV_a for the region of the pressure dependence dominated by ligand dissociation was 69 mL/mol, an unexpectedly large value. For tetramer modified with methyl methanethiosulfonate, subunit dissociation was shifted to much higher pressures and IPTG dissociation did not occur. The ΔV_a for subunit association was calculated as ~160 mL/mol, and the $C_{1/2}$ was 3.5×10^{-9} M. Interactions at the subunit interface of the modified protein are apparently stronger than in the unmodified protein. The absence of inducer dissociation from the MMTS-modified tetramer by the application of high hydrostatic pressure suggests that the volume change for inducer binding to the modified protein is much smaller than that observed for the unmodified repressor.

Specific interactions between proteins and nucleic acids have become the subject of increasing interest in recent years due to their important role in the regulation of biological functions. In addition to those proteins that are directly involved in the processes of transcription, replication, and translation, several proteins involved in the regulation of these events have been studied. Examples of such proteins include the *lac*, *trp*, *gal*, Cro, and C_I repressors and the catabolite activator protein (Miller & Reznikoff, 1980; Freifelder, 1983). Because these proteins exist as oligomers in solution, the equilibria involved in their specific DNA interactions include not only those of the nucleic acid and the effector molecules binding to the oligomer but also the interactions between the individual protein subunits. Although protein–DNA interactions have been examined in some detail (Miller & Reznikoff, 1980; Cold Spring Harbor Symposium, 1982; Ohlendorf & Matthews, 1983; Watson, 1983), the protein–protein interactions have not been adequately characterized due to the relatively high affinity between the subunits.

The lactose repressor protein controls expression of the metabolic enzymes for the *lac* operon by specific interaction at the operator site in the genome (Miller & Reznikoff, 1980). Binding to this site is modulated by interaction of sugar ligands with the tetrameric repressor protein (M_r 150 000); inducers decrease the affinity of the protein for operator DNA, while anti-inducers stabilize the repressor–operator complex (Miller & Reznikoff, 1980). The alterations in operator affinity elicited by these ligands are mediated by conformational changes in the repressor protein structure (Miller & Reznikoff, 1980). The binding of inducer to the free repressor protein is noncooperative at neutral pH but is cooperative (Hill coefficient = 1.4) in the presence of 40-bp[1] operator DNA fragments (O'Gorman et al., 1980). This cooperativity presumably reflects subunit–subunit interactions that influence the inducer binding behavior of the protein when complexed with its target

† This work was supported by grants from the National Institutes of Health (GM 11223 to G.W. and GM 22441 to K.S.M.) and the Robert A. Welch Foundation (C-576 to K.S.M.). T.J.D. was an NIH predoctoral trainee (GM 07833).
* Author to whom correspondence should be addressed.
‡ Present address: Tour 42-43, Université de Paris VII, UER de Biochemie, 75005 Paris, France.

[1] Abbreviations: ABP, arabinose binding protein; bp, base pair; DTE, dithioerythritol; IPTG, isopropyl β-D-thiogalactoside; MMTS, methyl methanethiosulfonate; SDS, sodium dodecyl sulfate.

0006-2960/86/0425-8308$01.50/0